Lumped Parameter Modeling of Organic Solar Cells' S-Shaped *I–V* Characteristics

Francisco J. García-Sánchez, *Senior Member, IEEE*, Denise Lugo-Muñoz, *Member, IEEE*, Juan Muci, and Adelmo Ortiz-Conde, *Senior Member, IEEE*

***Abstract*—This paper addresses lumped parameter equivalent circuit modeling of the S-shape anomaly observed in many experimental organic solar cells' *I–V* characteristics measured under illumination. It presents a convenient exact analytic expression for the cell's terminal voltage as an explicit function of its terminal current according to a model previously proposed by other authors. A new model is also recommended here in order to improve the previous model so that it may also describe the exponential-like upward bend observed at large forward voltages in the first quadrant of the *I–V* characteristics beyond the S-shape kink. The explicit nature of the proposed equations avoids numerical iteration and eases fitting to experimental data when extracting the cell's model parameters. It also facilitates the derivation of other analytic expressions, such as the temperature dependence of the open-circuit voltage.**

***Index Terms*—Organic solar cells (OSCs), solar cell modeling, s-shaped "kink".**

I. Introduction

ORGANIC solar cells (OSCs), which are fabricated using both polymers and small organic molecules, represent a very attractive low-cost alternative for many photovoltaic applications. They can be directly deposited as flexible lightweight films over arbitrarily shaped surfaces by a variety of simple and inexpensive printing or coating techniques. Nevertheless, OSCs have yet to attain conversion efficiencies that would make them competitive. Therefore, substantial basic research and development is still needed in OSC materials, structures, and processing techniques. The analysis of the cells' current–voltage (*I–V*) characteristics under illumination is obviously an essential tool for this task [1].

Many still unoptimized developmental OSCs exhibit anomalous S-shaped "kinks" in their *I–V* characteristics [2], probably caused by contact and other interface phenomena [3]. The occurrence of this anomalous "kink" also seems to be dependent on fabrication and postdeposition treatment. This S-shape shows up in illuminated *I–V* characteristics' fourth quadrant, significantly reducing the fill factor and thereby decreasing the cell's overall conversion efficiency. One typical example of such behavior are OSCs based on P3HT:PCBM donor–acceptor interfaces [4].

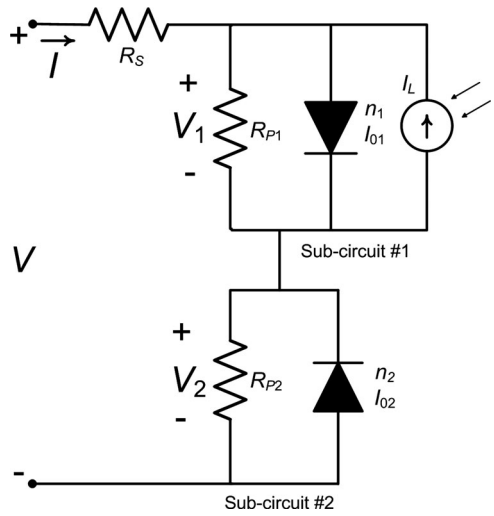

Fig. 1. Previously proposed OSC lumped parameter equivalent circuit model [6], including a conventional single-diode solar cell equivalent subcircuit #1 in series with an anomalous S-shape producing subcircuit #2.

Including this anomalous behavior in OSC lumped parameter modeling enables quantitative analysis of its emergence and evolution. To that end, extra lumped components are usually added to a conventional solar cell lumped parameter equivalent circuit model, extending its descriptive ability to include anomalous behavior [5]. In particular, a modified version of the conventional single-diode solar cell equivalent circuit has recently been proposed to account for the anomalous S-shaped "kink" observed in many OSC *I–V* characteristics [6]. This modified model incorporates a series-connected additional circuit, consisting of a parallel combination of a reverse-connected diode and a shunt resistance, as shown in Fig. 1.

II. Previous Model

The already proposed equivalent circuit model [6], which is presented in Fig. 1, specifies that the OSC terminal voltage is given by the sum of the voltages of three series-connected subcircuits

$$V = V_R + V_1 + V_2. \tag{1}$$

On the other hand, the terminal current flowing through the series-connected subcircuits is given by either one of the

Manuscript received July 24, 2012; revised September 4, 2012; accepted September 13, 2012. Date of publication October 9, 2012; date of current version December 19, 2012.

The authors are with the Solid State Electronics Laboratory, Simón Bolívar University, Caracas 1080, Venezuela (e-mail: fgarcia@ieee.org; denise267@gmail.com; jmuci@usb.ve; ortizc@ieee.org).

Color versions of one or more of the figures in this paper are available online at http://ieeexplore.ieee.org.

Digital Object Identifier 10.1109/JPHOTOV.2012.2219503

following three equations:

$$I = \frac{V_R}{R_S} \tag{2}$$

$$I = I_{01}\left(e^{\frac{V_1}{n_1 v_t}} - 1\right) + \frac{V_1}{R_{P1}} - I_L \tag{3}$$

$$I = -I_{02}\left(e^{-\frac{V_2}{n_2 v_t}} - 1\right) + \frac{V_2}{R_{P2}} \tag{4}$$

where I_{01} and I_{02} are the reverse currents, n_1 and n_2 are the ideality factors, v_t is the thermal voltage $= k_B \mathrm{T}/q$, and I_L is the photogenerated current. Note that only subcircuit #1 is supposed to be affected by the illumination in this equivalent circuit model scheme.

The above four equations constitute a transcendental system of equations from which the terminal current or voltage has formerly been solved either by numerical methods [4] or using approximations [6]. Approximate solutions involve neglecting some of the currents with respect to the total current [6]. However, doing so unfortunately often produces unacceptable errors at the time of model parameter extraction [4]. Numerical solutions, on the other hand, can yield correct results to any arbitrary precision, but unavoidably entail cumbersome algorithms and time-consuming iterations [4]. Moreover, nonexplicit model equations do not favor performing analytic operations such as integration or differentiation which are frequently useful in obtaining other expressions for derived variables.

We propose to circumvent the shortcomings, of having to resort to approximate and numerical solutions to calculate the terminal voltage, by making use of an explicit form of the terminal voltage (1). Such a solution may be obtained by explicitly solving V_1 and V_2 from (3) and (4), respectively. This can be accomplished by the use of the Lambert W function [7], which is a special function commonly used nowadays in semiconductor device modeling. Solving (3) and (4) in this manner, V_1 and V_2 are then given explicitly by

$$V_1 = n_1\, v_t\, \ln\left[\frac{n_1 v_t}{R_{P1} I_{01}} W_0\left(\frac{R_{P1} I_{01}}{n_1 v_t} e^{\frac{R_{P1}(I + I_{01} + I_L)}{n_1 v_t}}\right)\right] \tag{5}$$

and

$$V_2 = -\, n_2\, v_t\, \ln\left[\frac{n_2 v_t}{R_{P2} I_{02}} W_0\left(\frac{R_{P2} I_{02}}{n_2 v_t} e^{-\frac{R_{P1}(J - J_{02})}{n_1 v_t}}\right)\right]. \tag{6}$$

Substitution of the above solutions into (1) results in the terminal voltage being expressed in closed form as

$$V = IR_S + v_t\, \ln\left\{\frac{\left[\frac{n_1}{R_{P1} I_{01}} W_0\left(\frac{R_{P1} I_{01}}{n_1 v_t} e^{\frac{R_{P1}(I + I_{01} + I_L)}{n_1 v_t}}\right)\right]^{n_1}}{\left[\frac{n_2}{R_{P2} I_{02}} W_0\left(\frac{R_{P2} I_{02}}{n_2 v_t} e^{-\frac{R_{P2}(I - I_{02})}{n_2 v_t}}\right)\right]^{n_2}}\right\} \tag{7}$$

where W_0 stands for the principal branch of the Lambert W function [7].

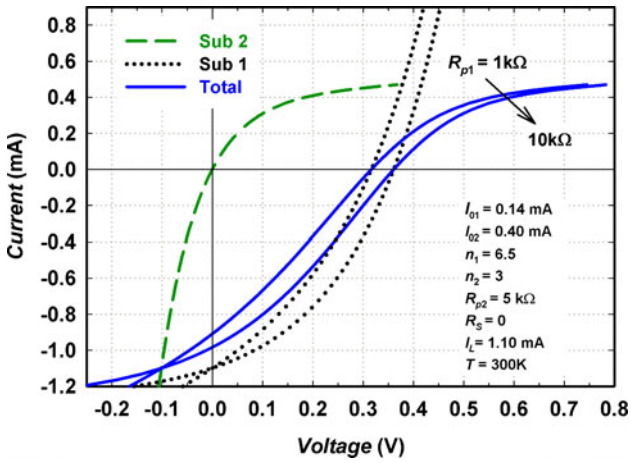

Fig. 2. Synthetic S-shaped *I–V* characteristics of a hypothetical OSC under illumination (solid lines), calculated using (7) according to the previous model [6], for two values of shunt resistance R_{P1}. The characteristics of subcircuit #1 (dotted lines) and S-shape anomaly producing subcircuit #2 (dashed line) are also shown for completeness.

Therefore, (7) now describes the terminal voltage of the illuminated OSC with anomalous S-shaped *I–V* characteristics as an analytical explicit function of the cell's terminal current. Unfortunately, an analytical solution for the terminal current as an explicit function of the terminal voltage is not feasible in this case. Despite this, (7) is still very useful since it avoids approximations or iterative numerical procedures. Moreover, lateral fitting [8] may be used for parameter extraction purposes, by directly fitting (7) to the measured illuminated *V–I* data. Furthermore, (7) may be analytically differentiated with respect to its internal parameters to explicitly describe some type of variability, for example, to find the open-circuit voltage temperature dependence.

The use of the presently proposed explicit voltage (7) allows us to quickly analyze the effect of the various model parameters on the cell's *I–V* characteristics. As an example, Fig. 2 illustrates the effect of changing the shunt resistance R_{P1} of subcircuit #1 (which represents the traditional one-diode solar cell model) on the total OSC S-shaped illuminated *I–V* characteristics. In this case, instead of using numerical iteration, the total *V–I* characteristics were directly calculated according to the previous OSC model [6], using the presently proposed explicit voltage (7) with the parameters indicated in the figure's inset. The parameter values used are comparable with those recently extracted from experimental OSCs [4]. The value of the series resistance R_S was kept zero in Fig. 2 so as not to obscure the comparison. We note that, as expected, the effect of reducing R_{P1} is to decrease the short-circuit current as well as the open-circuit voltage of the total illuminated OSC *I–V* characteristics.

III. Proposed New Model

Many developmental OSCs while still in the experimental stage often exhibit under illumination a further exponential-like rise of the current in the first quadrant of their already anomalous S-shaped *I–V* characteristics for voltages $\gg V_{\mathrm{OC}}$ [3], [6], [9]–[16]. In such cases, the previously proposed equivalent circuit

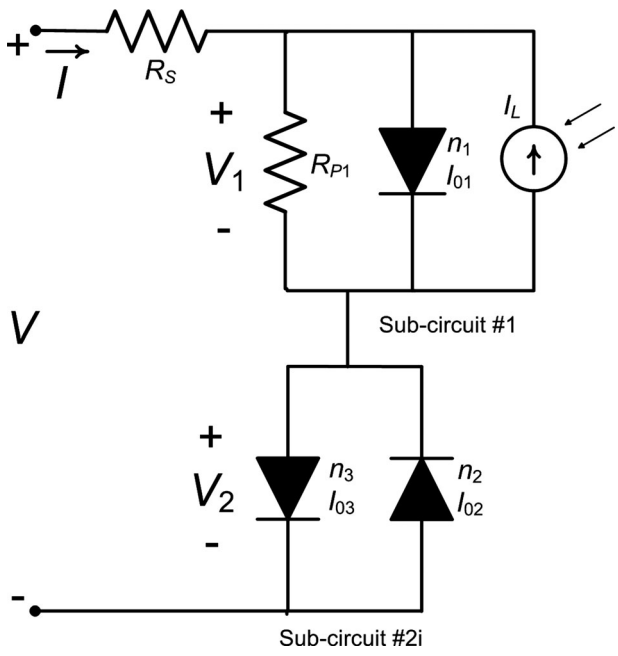

Fig. 3. Presently proposed improved lumped parameter equivalent circuit model for OSCs. The anomalous S-shape producing subcircuit #2i, in series with the conventional single-diode solar cell equivalent subcircuit #1, now contains a third forward-connected diode replacing R_{P2}.

[6] in Fig. 1, as well as its ensuing explicit voltage (7) presented above, provides an adequate description of the S-shaped part of the *I–V* characteristics, but it is incapable of representing the distinct additional current increase beyond the S-shaped kink feature. The reason is that the first quadrant $(V > V_{\rm OC})$ in the previously proposed model is primarily dominated by the linear element R_{P2}, and thus, the *I–V* relationship turns out to be quasi-linear for large forward voltages $\gg V_{\rm OC}$.

In order to include a proper description of such a shape, we propose to improve the previous model by replacing subcircuit #2's shunt resistance R_{P2} by another diode with n_3 and I_{03}, but this time connected in the forward direction, as indicated in subcircuit #2i of Fig. 3. This substitution modifies the current through the anomalous S-shape producing subcircuit, which instead of being given by (4) is now described by

$$I = -I_{02}\left(e^{-\frac{V_2}{n_2 v_t}} - 1\right) + I_{03}\left(e^{\frac{V_2}{n_3 v_t}} - 1\right). \tag{8}$$

We would like to explicitly solve the above equation for the voltage, but that is impossible in general. However, there are cases when an explicit solution for V_2 is easily obtainable from (8): *case a* if n_3 and n_2 have equal value; and *case b* if n_3 is equal to twice n_2. In general, (8) would have to be solved numerically for the terminal voltage, as formerly done.

In case a, letting $n_3 = n_2$, the voltage V_{2a} at the terminals of the S-shape producing subcircuit #2i is

$$V_{2a} = n_2\, v_t\, \ln\left[\frac{I - I_{02} + I_{03}}{2I_{03}} + \sqrt{\left(\frac{I - I_{02} + J_{03}}{2I_{03}}\right)^2 + \frac{I_{02}}{I_{03}}}\right]. \tag{9}$$

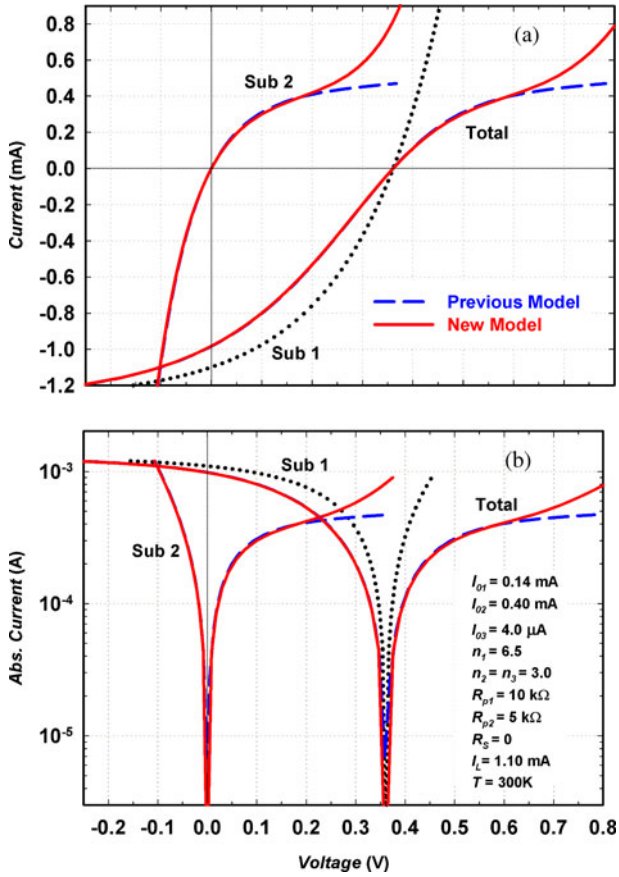

Fig. 4. *I–V* characteristics in (a) linear and (b) semi-log scales of a hypothetical OSC under illumination, using the previous model of Fig. 1 (dashed lines), and the presently proposed model of Fig. 3 (solid lines). The conventional subcircuit #1 characteristics (dotted lines) are also shown as reference.

In case b, letting $n_3 = 2n_2$, the voltage V_{2b} at the terminals of the S-shape producing subcircuit #2 is

$$V_{2b} = 2\, n_2 v_t \ln \times \left\{\frac{1}{3I_{03}}\left|\frac{f}{2} + \frac{2\left(I_{02} - I_{03} - I\right)^2}{f} - \left(I_{02} - I_{03} - I\right)\right|\right\} \tag{10}$$

where

$$f = \Big[108 I_{02} I_{03}^2 - 8\left(I_{02} - I_{03} - I\right)^3 + 12\sqrt{3}\sqrt{-I_{02}\left[(-27 I_{02} I_{03}^2) + 4\left(I_{02} - I_{03} - I\right)^3\right] I_{03}}\Big]^{1/3}. \tag{11}$$

Using (1), we can now add V_R, from (2), V_1, from (5), and either V_{2a} or V_{2b}, from (9) or (10) as the case might be, to obtain the terminal voltage of the illuminated OSC expressed as an explicit function of its current according to the presently proposed new model.

Fig. 4 presents a comparison of the new model's playback with $n_3 = n_2$ (case a), using (9) in (1) to describe V_{2a}, to that of the previous model using (7). As is evident from the figure, the

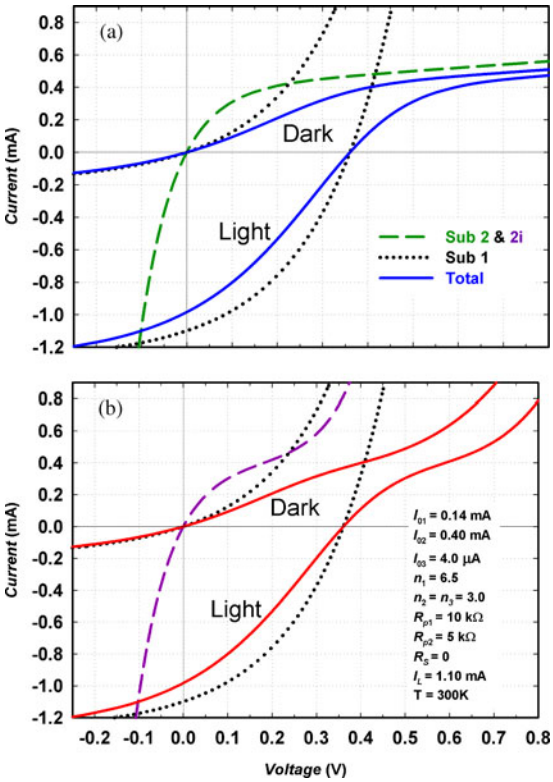

Fig. 5. Dark and illuminated *I–V* characteristics obtained from (a) the previous model and (b) the proposed new model. The characteristics of subcircuit #1 (dotted line) and those of subcircuits #2 and 2i (dashed lines) are also included as reference.

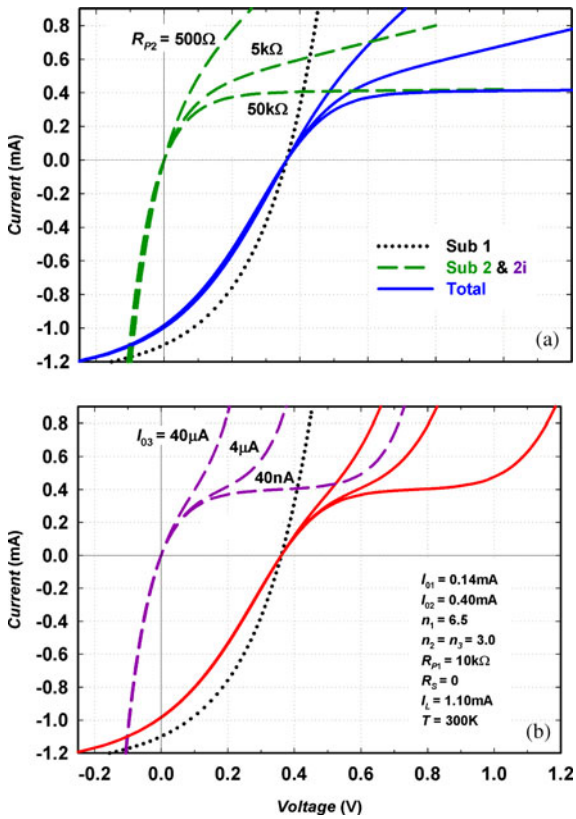

Fig. 6. Effect on the *I–V* characteristics of changing the shunt resistance R_{P2} in the previous model (a), and changing the reverse current I_{03} in the new model (b). The characteristics of subcircuit #1 (dotted line) and those of subcircuits #2 and 2i (dashed lines) are also included as reference.

main difference introduced by the presence of the third diode in the new model is that the resulting S-shaped *I–V* characteristics are now allowed to bend up in the first quadrant for large forward voltages.

As mentioned before, the previous model forces the current to grow in a linear-like manner, whereas the new model allows the current to grow exponentially in the first quadrant. This extra diode in the new model accommodates the additional feature seen in the first quadrant of many experimental OSC *I–V* characteristics [6], [9]–[16].

The total illuminated *I–V* characteristics of the OSC cannot be obtained by simply shifting its total dark *I–V* characteristics. Rather, since illumination only affects subcircuit #1, only its *I–V* characteristics are down shifted by an amount equal to I_L, but subcircuit #2, or #2i, in the case of the new model, is left unchanged. Fig. 5 clearly illustrates this fact by showing synthetic dark and illuminated OSC *I–V* characteristics according to both the previous model (top) and the proposed new model (bottom).

IV. Discussion

To further visualize the capabilities of the proposed model, we will next analyze how changing the values of the parameters in both models affects the shape of the resulting OSC *I–V* characteristics. To that effect, we will use case a of the presently proposed model, that is, we will let $n_3{=}n_2$ to calculate V_{2a} using (9). The shunt resistance $R_{P\,2}$ and the reverse current I_{02} of subcircuit #2 in the previous model, and the reverse currents I_{02} and I_{03} of subcircuit #2i in the new model, will be adjusted to illustrate their effect.

Fig. 6 shows the S-shaped illuminated *I–V* characteristics for three subcircuit #2 shunt resistance $R_{P\,2}$ values in the previous model (top), and for three values of the reverse current I_{03} in subcircuit #2i of the proposed new model (bottom). The figure illustrates how both parameters control the severity of the anomalies.

Fig. 7 shows the effect of changing the value of subcircuit #2's reverse current I_{02}. Its value determines the location of the convexity in the S-shaped anomaly for both the previous model (top) and the new model (bottom).

Therefore, by properly choosing parameters I_{02} and $R_{P\,2}$ in subcircuit #2 of the previous model, or I_{02} and I_{03} in subcircuit #2i of the new model, we have an ample range of possible combinations to describe the S-shaped anomaly and the current upward turn that might be present beyond $V_{\rm OC}$. Of course, the diode quality factors n_1, n_2, and n_3 may be also adjusted to best fit the measured data.

To validate the ability of the presently proposed improved lumped parameter model of Fig. 3 to describe the anomalous S-shape "kink" together with the additional upward exponential rise of the current in the first quadrant of real OSCs, we used it to describe the recently proposed *I–V* characteristics

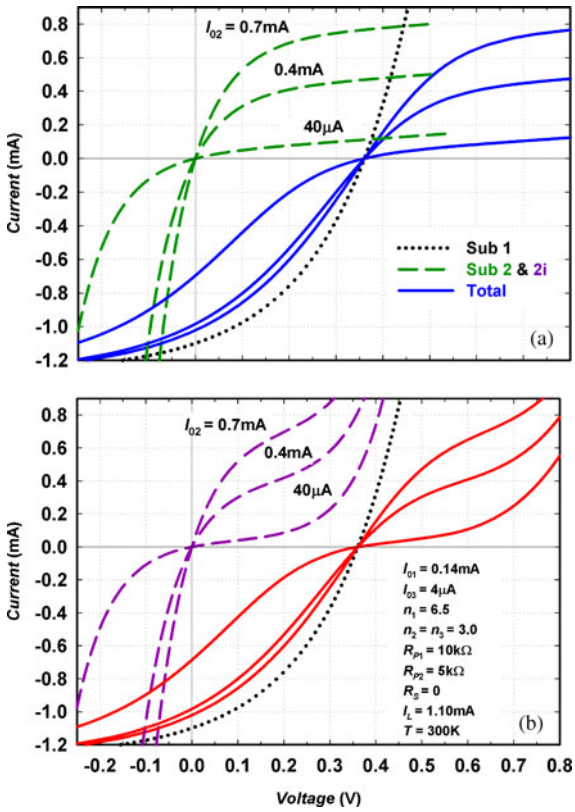

Fig. 7. Effect on the *I–V* characteristics of changing the reverse current I_{02} in the previous model (a) and in the proposed new model (b). The characteristics of subcircuit #1 (dotted line) and those of subcircuits #2 and 2i (dashed lines) are also included as reference.

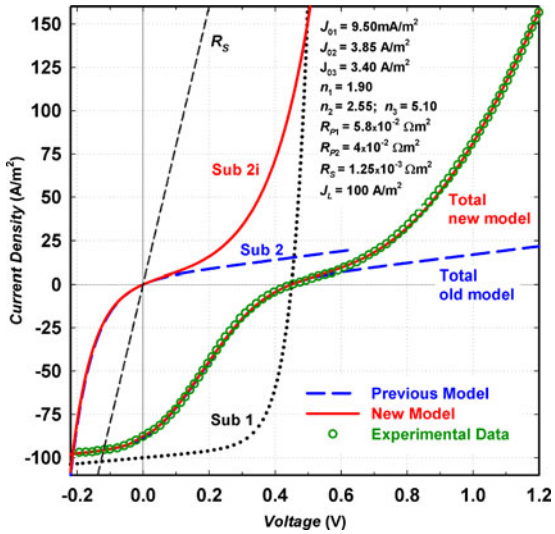

Fig. 8. Measured data (symbols) of an experimental OSC [10] under illumination, shown together with the previous and the new models' *I–V* characteristics playbacks. The characteristics of the series resistance (short-dashed line), subcircuit #1 (dotted line), and subcircuits #2 and 2i (long-dashed lines) are also included as reference.

measured under illumination of an experimental bulk heterojunction P3HT:PCBM OSC [10]. The data points used correspond to the particular device without a PEDOT:PSS layer subjected to an oxygen plasma treatment during a time of 100 s [10].

For this cell, we used case b ($n_3 = 2n_2$) of subcircuit #2i with its terminal voltage V_{2b} given by (10). Fig. 8 presents the measured data together with the model playback, using the parameters indicated in the figure's inset. Also shown in that figure is the inadequate playback of the previous model, as calculated with (7). In contrast, the new model adequately reproduces the observed shape up to large values of forward voltage, whereas the previously proposed model is able to do so only up to about voltages slightly above $V_{\rm OC}$ (<0.6 V).

V. Conclusion

The two improvements to the previous OSC's lumped parameter model [6] include: 1) an explicit form of the model's terminal voltage equation to optimize calculations and parameter extraction; and 2) an improvement of the previous model by replacing the shunt resistor ($R_{p\,2}$ in Fig. 1) with a diode (n_3 in Fig. 3), in order to describe the additional upward bend observed in the first quadrant beyond the anomalous S-shape "kink" of illuminated *I–V* characteristics, which was not accounted for by the previous model. Such a replacement might suggest a possible physical origin of the observed anomalous upward bend behavior.

The proposed terminal voltage equations presented for the previous model, as well as for the new one, are explicit in nature. As such, the need for numerical iteration is avoided, and procedures used to extract model parameters by fitting the voltage equations to data can be considerably simplified. The explicit equations also facilitate analytic differentiation and integration.

Further improvement of this model is possible by letting subcircuit #1 assume a multiexponential form [17]. However, such improvement, as well as allowing n_2 and n_3 to take arbitrary values, could render the lumped parameter circuit's equations explicitly unsolvable, and thus, numerical iteration methods would have to be used again.

References

[1] G. Li, L. Liu, F. Wei, S. Xia, and X. Qian, "Recent progress in modeling, simulation, and optimization of polymer solar cells," *IEEE J. Photovoltaics*, vol. 2, no. 3, pp. 320–340, Jul. 2012.

[2] H. Mori, E. Miyazaki, I. Osaka, and K. Takimiya, "Organic photovoltaics based on 5-hexylthiophene-fused porphyrazines," *Organic Electron.*, vol. 13, pp. 1975–1980, 2012.

[3] J. Wagner, M. Gruber, A. Wilke, Y. Tanaka, K. Topczak, A. Steindamm, U. Hörmann, A. Opitz, Y. Nakayama, H. Ishii, J. Pflaum, N. Koch, and W. Brütting, "Identification of different origins for s-shaped current voltage characteristics in planar heterojunction organic solar cells," *J. Appl. Phys.*, vol. 111, no. 5, pp. 054509-1–054509-12, 2012.

[4] F. Araujo de Castro, J. Heier, F. Nüesch, and R. Hany, "Origin of the kink in current-density versus voltage curves and efficiency enhancement of polymer-C_{60} heterojunction solar cells," *IEEE J. Sel. Topics Quantum Electron.*, vol. 16, no. 6, pp. 1690–1699, Nov./Dec. 2010.

[5] B. Mazhari, "An improved solar cell circuit model for organic solar cells," *Solar Energy Mater. Solar Cells*, vol. 90, pp. 1021–1033, 2006.

[6] G. del Pozo, B. Romero, and B. Arredondo, "Evolution with annealing of solar cell parameters modeling the S-shape of the current–voltage characteristic," *Solar Energy Mater. Solar Cells*, vol. 104, pp. 81–86, 2012.

[7] R. M. Corless, G. H. Gonnet, D. E. G. Hare, D. J. Jeffrey, and D. E. Knuth, "On Lambert W function," *Adv. Comput. Math.*, vol. 5, no. 1, pp. 329–359, 1996.

[8] A. Ortiz-Conde, Y. Ma, J. Thomson, E. Santos, J. J. Liou, F. J. García-Sánchez, M. Lei, J. Finol, and P. Layman, "Direct extraction of semicon-

ductor diode parameters using lateral optimization method," *Solid-State. Electron.*, vol. 43, pp. 845–848, 1999.

[9] A. Kumar, S. Sista, and Y. Yanga, "Dipole induced anomalous S-shape I-V curves in polymer solar cells," *J. Appl. Phys.*, vol. 105, pp. 094512-1–094512-6, 2009.

[10] A. Wagenpfahl, D. Rauh, M. Binder, C. Deibel, and V. Dyakonov, "S-shaped current-voltage characteristics of organic solar devices," *Phys. Rev. B*, vol. 82, p. 115306, 2010.

[11] J. C. Wang, X. C. Ren, S. Q. Shi, C.W. Leung, and P. K. L. Chan, "Charge accumulation induced S-shape J–V curves in bilayer heterojunction organic solar cells," *Organic Electron.*, vol. 12, pp. 880–885, 2011.

[12] L. He, C. Jiang, H. Wang, D. Lai, and Rusli, "High efficiency planar Si/organic heterojunction hybrid solar cells," *Appl. Phys. Lett.*, vol. 100, no. 7, pp. 073503-1–073503-3, 2012.

[13] Y. Matsuo, A. Ozu, N. Obata, N. Fukuda, H. Tanaka, and E. Nakamura, "Deterioration of bulk heterojunction organic photovoltaic devices by a minute amount of oxidized fullerene," *Chem. Commun.*, vol. 48, pp. 3878–3880, 2012.

[14] J. Ge, J. Liu, X. Guo, Y. Qin, H. Luo, Z.-X. Guo, and Y. Li, "Photovoltaic properties of dimeric methanofullerenes containing hydroxyl groups," *Chem. Phys. Lett.*, vol. 535, pp. 100–105, 2012.

[15] N. Wang, J. Yu, Y. Zheng, Z. Guan, and Y. Jiang, "Organic photovoltaic cells based on a medium-bandgap phosphorescent material and C_{60}," *J. Phys. Chem. C*, vol. 116, pp. 5887–5891, 2012.

[16] N. K. Elumalai, L. M. Yin, V. Chellappan, Z. Jie, Z. Peining, and S. Ramakrishna, "Effect of C_{60} as an electron buffer layer in polythiophene methanofullerene based bulk heterojunction solar cells," *Phys. Status Solidi A*, pp. 1–6, 2012.

[17] A. Ortiz-Conde, D. Lugo-Muñoz, and F. J. García-Sánchez, "An explicit multiexponential model as an alternative to traditional solar cell models with series and shunt resistances," *IEEE J. Photovoltaics*, vol. 2, no. 3, pp. 261–268, Jul. 2012.

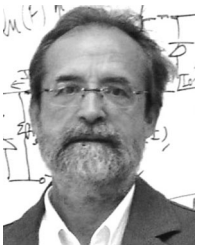

Francisco J. García-Sánchez (M'76–SM'97) was born in Madrid, Spain. He received the B.E.E., M.E.E., and Ph.D. degrees in electrical engineering from the Catholic University of America, Washington, DC, in 1970, 1972, and 1976, respectively.

In 1977, he joined the faculty of the Electronics Department, Universidad Simón Bolívar (USB), Caracas, Venezuela, where he became a Full Professor in 1987. He has conducted research on polycrystalline solar cell fabrication and semiconductor device modeling. He has contributed to more than 170 articles in refereed technical journals and conferences, has co-authored a book on modeling, and has been editor of several specialized collective works.

Dr. García-Sánchez is currently a member of the IEEE Electron Devices Society (EDS) Master and Ph.D. Student Fellowships Committee, and is the EDS Newsletter's Region 9 Editor. He has received several awards for excellence in research. He has been an EDS Distinguished Lecturer since 2003. In 2007, he was conferred the honorary title of Professor Emeritus of USB.

Denise Lugo-Muñoz (M'11) was born in Punto Fijo, Venezuela. She received the Professional Electronics Engineer degree in 2009 and the Magister of Electronics Engineering degree (Hons.), majoring in solid-state electronics, in 2011, both from Simón Bolívar University (USB), Caracas, Venezuela, where she is currently working toward the D.Eng. degree. She graduated "*Cum Laude*" from her undergraduate engineering studies.

Since 2009, she has been working as a Research Assistant with the Solid State Electronics Laboratory, USB, where she has carried out research activities in the areas of physics-based modeling, simulation and parameter extraction of MOSFETs, p-i-n diodes, and solar cells. She is a coauthor of several articles published in technical journals and specialized conferences.

Ms. Lugo-Muñoz received the Outstanding Master's Thesis Award.

Juan Muci was born in Valencia, Venezuela. He received the Professional Electronics Engineer degree in electronics engineering from Simón Bolívar University (USB), Caracas, Venezuela, in 1979 and the M.S. degree in electrical engineering from Pennsylvania State University, State College, where he worked on gated diode modeling, until 1983.

He later joined the Electronics Department faculty at USB, where he is currently a Full Professor and is currently the Head of the Solid State Electronics Laboratory. He has authored numerous articles in technical journals and specialized conferences. His research interests include semiconductor device modeling and characterization.

Prof. Muci is a member of Tau Beta Pi and Eta Kappa Nu.

Adelmo Ortiz-Conde (S'82–M'85–SM'97) was born in Caracas, Venezuela. He received the Professional Electronics Engineer degree from Simón Bolívar University (USB), Caracas, in 1979 and the M.E. and Ph.D. degrees from the University of Florida, Gainesville, in 1982 and 1985, respectively.

In 1985, he joined the technical Staff of Bell Laboratories, Reading, PA, where developed high-voltage integrated circuits. In 1987, he rejoined the Electronics Department, USB, where he was promoted to Full Professor in 1995. He has coauthored a textbook and more than 160 international technical journal and conference articles (including 15 invited review articles). His current research interests include the modeling and parameter extraction of semiconductor devices.

Prof. Ortiz-Conde is an IEEE Electron Devices Society Distinguished Lecturer and the Chair of IEEE's Circuits and Systems/Electron Devices Venezuelan Joint Chapter. He is the Editor of IEEE ELECTRON DEVICE LETTERS in the area of silicon devices and technology.